Journal of Alloys and Compounds 750 (2018) 996–1002

Contents lists available at ScienceDirect

Journal of Alloys and Compounds

journal homepage: http://www.elsevier.com/locate/jalcom

Crystal structure, phase composition and microwave dielectric properties of $Ca_3MSi_2O_9$ ceramics

Xiao-Qiang Song [a, b], Kang Du [a, b], Xian-Zhe Zhang [a], Jie Li [a, b], Wen-Zhong Lu [a, b], Xiao-Chuan Wang [a, b], Wen Lei [a, b, c, *]

[a] School of Optical and Electronic Information, Huazhong University of Science and Technology, Wuhan, 430074, PR China
[b] Key Lab of Functional Materials for Electronic Information (B), Ministry of Education, Wuhan, 430074, PR China
[c] Engineering Research Center for Functional Ceramics, Ministry of Education, Wuhan, 430074, PR China

ARTICLE INFO

Article history:
Received 4 January 2018
Received in revised form
23 March 2018
Accepted 4 April 2018
Available online 7 April 2018

Keywords:
Cuspidine structure
Phase composition
Microwave dielectric properties

ABSTRACT

$Ca_3MSi_2O_9$ (M = Zr, Hf, $Sn_{1-x}Ti_x$; x = 0–0.40) low-permittivity microwave dielectric ceramics with cuspidine structure were prepared using conventional solid-state method at 1325 °C–1400 °C for 10 h in air. The lattice parameters of $Ca_3MSi_2O_9$ (*CMS*) linearly decreased when M changed from Zr to $Sn_{0.85}Ti_{0.15}$, and a single phase was formed. For $M = Sn_{1-x}Ti_x$ (x = 0.20–0.40), a second phase of $CaTiO_3$ (CT) appeared. The relative permittivity (ε_r), quality factor ($Q \times f$), and temperature coefficient of resonant frequency (τ_f) were closely related to ionic polarizability, relative covalence of M site, unit-cell volume, and $CaTiO_3$ second phase. As a result, the highest $Q \times f$ value of 72840 GHz was obtained for $M = Sn_{0.95}Ti_{0.05}$, and near zero τ_f value was achieved for $M = Sn_{0.7}Ti_{0.30}$. The microwave dielectric properties of which are as follows: ε_r = 11.07, $Q \times f$ = 42400 GHz, and τ_f = −5.1 ppm/°C.

1. Introduction

High-performance microwave dielectric ceramics with low permittivity have attracted considerable attention due to the expansion of the operating frequency ranges of microwave wireless communication. Low-permittivity ($\varepsilon_r < 15$) microwave dielectric ceramics can be used as high-frequency substrates, dielectric antennas, high-accuracy capacitors, and millimeter-wave components such as resonators and filters [1]. This kind of ceramics is the foundation of the microwave wireless communication. For practical applications, such microwave dielectric ceramics must have a low dielectric constant (ε_r) to reduce the signal transmit delay, a high-quality factor ($Q \times f$) for frequency selectivity, and a near-zero temperature coefficient of resonant frequency (τ_f) for stability of the transmitted frequency [2,3].

Silicates exhibit some interesting characteristics, such as ferroelectricity in Bi_2SiO_5 and $BaZnSiO_4$ [1,4], unusual thermal expansion coefficient in $Ba_{1-x}Sr_xZn_2Si_2O_7$ [5], and microwave dielectric properties in Sm_2SiO_5 [6]. These interesting phenomena are related to the complex crystal structure of silicates, which are constituted by [SiO_4] tetrahedrons and some other polyhedrons. Usually, silicates have a low permittivity value due to the Si–O bond, which contains 45% ionic bond and 55% covalent bond [6]. Many kinds of silicates have been explored, such as forstreite (Mg_2SiO_4), willemite (Zn_2SiO_4), and cuspidine ($Ca_3MSi_2O_9$, M = Zr and Sn) [7–9]. All of them have a low permittivity value and high quality factor, making them a good choice for millimeter-wave devices. However, their τ_f value exhibits generally a negative value. Moreover, Mg_2SiO_4 and Zn_2SiO_4 are difficult to obtain a single phase, and cold isostatic processing is required during molding [10–12]. Cuspidine-type $Ca_3ZrSi_2O_9$ ceramic possesses a stable crystal structure, and the solid solution can be achieved by substitution of Zr^{4+} ions to improve microwave dielectric properties [9]. Akinori Kan et al. [9] found that the cuspidine-type $Ca_3(Zr_{1-x}Sn_x)Si_2O_9$ solid solutions, which constitutes the [Si_2O_7] group, [$Zr_{1-x}Sn_xO_6$] octahedron, and [$CaO_{6/7}$] polyhedron, exhibited excellent low-permittivity microwave dielectric properties. When the Zr^{4+} was substituted by Sn^{4+}, the ε_r value decreased slightly, the $Q \times f$ value showed an increasing trend, and the τ_f value approached to zero. This results could be related closely to ionic polarizability and relative covalence at M site in $Ca_3MSi_2O_9$ lattice structure.

To clarify the effects of the M-site ions on the microwave dielectric properties and establish the relationships between lattice

* Corresponding author. School of Optical and Electronic Information, Huazhong University of Science and Technology, Wuhan, 430074, PR China.
E-mail address: wenlei@mail.hust.edu.cn (W. Lei).

https://doi.org/10.1016/j.jallcom.2018.04.044
0925-8388/

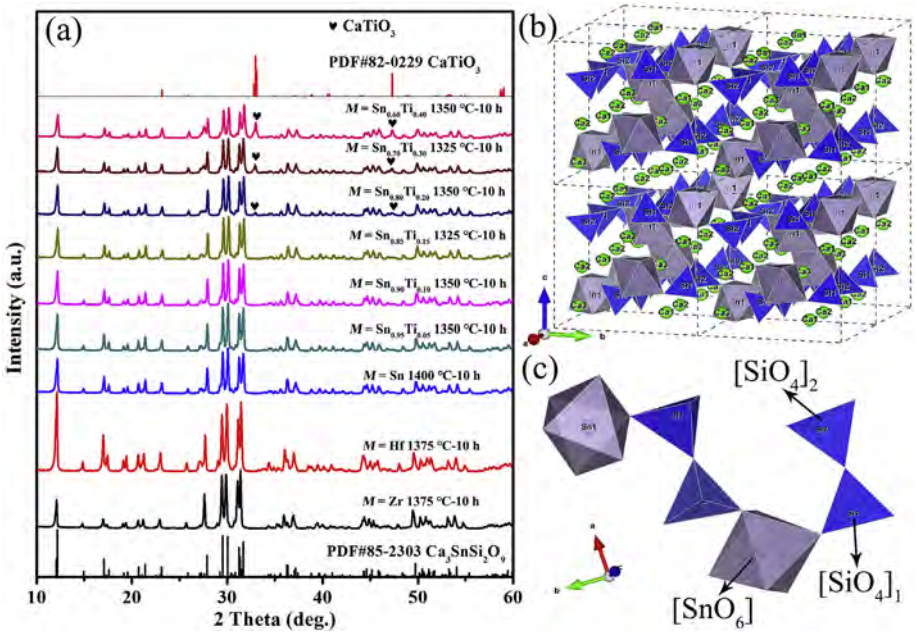

Fig. 1. (a) XRD patterns of $Ca_3MSi_2O_9$ (M = Zr, Hf, $Sn_{1-x}Ti_x$; x = 0–0.40) ceramics sintered at their optimum temperature, (b) crystal structure of $Ca_3MSi_2O_9$ (M = Sn) (2 × 2 × 2), and (c) [SnO_6]–[SiO_4] chain in unit cell for $Ca_3MSi_2O_9$ (M = Sn) ceramics.

Table 1
Lattice parameters and Rietveld discrepancy factors of $Ca_3MSi_2O_9$ (M = Zr, Hf, $Sn_{1-x}Ti_x$; x = 0–0.40) compositions.

Phase Composition	M	a (Å)	b (Å)	c (Å)	β (°)	V (Å^3)	Rwp (%)	Rp (%)	χ^2
CMS	Zr	7.360	10.178	10.442	90.898	782.059	6.90	5.00	4.09
	Hf	7.354	10.156	10.441	91.044	779.742	6.23	4.40	5.06
	Sn	7.321	10.067	10.429	91.073	768.351	6.87	5.03	3.67
	$Sn_{0.95}Ti_{0.05}$	7.318	10.066	10.427	91.078	768.099	6.78	4.83	3.62
	$Sn_{0.90}Ti_{0.10}$	7.312	10.065	10.423	91.079	766.976	6.98	5.00	3.67
	$Sn_{0.85}Ti_{0.15}$	7.307	10.060	10.415	91.091	765.467	6.97	5.22	3.75
CSS–CT	$Sn_{0.80}Ti_{0.20}$	7.306	10.060	10.414	91.090	765.305	7.32	5.46	4.01
	$Sn_{0.70}Ti_{0.30}$	7.306	10.062	10.414	91.081	765.432	7.93	5.82	4.50
	$Sn_{0.60}Ti_{0.40}$	7.301	10.056	10.409	91.100	764.063	12.16	8.73	9.41

parameters and microwave dielectric properties in the cuspidine-type $Ca_3MSi_2O_9$ solid solutions, several ions similar to Zr^{4+} and Sn^{4+} have to be selected to occupy the M site. Substitution of Ti^{4+} by Sn^{4+} [13] and Zr^{4+} [14] had been adopted to form a solid solution in the $Zn_2Ti_{1-x}Sn_xO_4$ and $Li_2Zn(Ti_{1-x}Zr_x)_3O_8$ microwave dielectric ceramics, respectively. In addition, Hf^{4+} exhibited similar characteristics to Zr^{4+} in the $ASiO_4$ (A = Zr, Hf) microwave dielectric ceramics [15,16]. Therefore, Zr^{4+}, Sn^{4+}, Ti^{4+}, and Hf^{4+} ions with the same valence state and similar ionic radii [17] could occupy the M site to form a cuspidine-type lattice structure in $Ca_3MSi_2O_9$ with a structural flexibility of [MO_6] octahedrons.

In this work, $Ca_3MSi_2O_9$ (M = Zr, Hf, Sn) ceramics and $Ca_3Sn_{1-x}Ti_xSi_2O_9$ (x = 0.05–0.40) solid solutions were prepared. The relationships among lattice parameters, phase composition, and microwave dielectric properties were investigated systematically.

2. Experimental procedure

The $Ca_3MSi_2O_9$ (M = Zr, Hf, $Sn_{1-x}Ti_x$; x = 0–0.40) ceramics were prepared by conventional solid-state method using reagent grade $CaCO_3$ (99.8%), SiO_2 (99.5%), ZrO_2 (99.5%), HfO_2 (99.5%), SnO_2 (99.5%), TiO_2 (99.5%) powder as raw materials. According to desired stoichiometry, the raw materials were weighed to ball milled in a polyethylene jar for 5 h using ZrO_2 balls with deionized water. After drying at 85 °C, the mixtures were calcined in air at 1000 °C for 3 h with a heat rate of 5 °C/min. And then the powders were uniaxially pressed into samples with dimensions of 12 mm in diameter and approximately 6 mm in height under a pressure of 150 MPa. The samples were sintered in the temperature range of 1325 °C–1400 °C for 10 h at a heating rate of 5 °C/min, and then they were naturally cooled in the furnace after being cooled to 1000 °C at a rate of 2 °C/min.

The bulk density of the sintered samples was measured by Archimedes' method. The relative density ρ_{rel} was obtained by:

$$\rho_{rel} = \frac{\rho_{obs}}{\rho_{the}} \times 100\ \% \quad (1)$$

where ρ_{obs} and ρ_{the} are the observed density and theoretical density, respectively.

For two-phase composite ceramics, ρ_{the} can be calculated by:

$$\rho_{the} = \frac{W_1 + W_2}{W_1/\rho_1 + W_2/\rho_2} \quad (2)$$

where W_1 and W_2 are the weight percentage of phase 1 and phase 2, and ρ_1 and ρ_2 are the theoretical density of phase 1 and phase 2, respectively.

X-ray diffraction (XRD) patterns were obtained using XRD (XRD-7000, Shimadzu, Kyoto, Japan) with CuKα radiation. The phase analysis was performed by Rietveld refinement [18] using GSAS

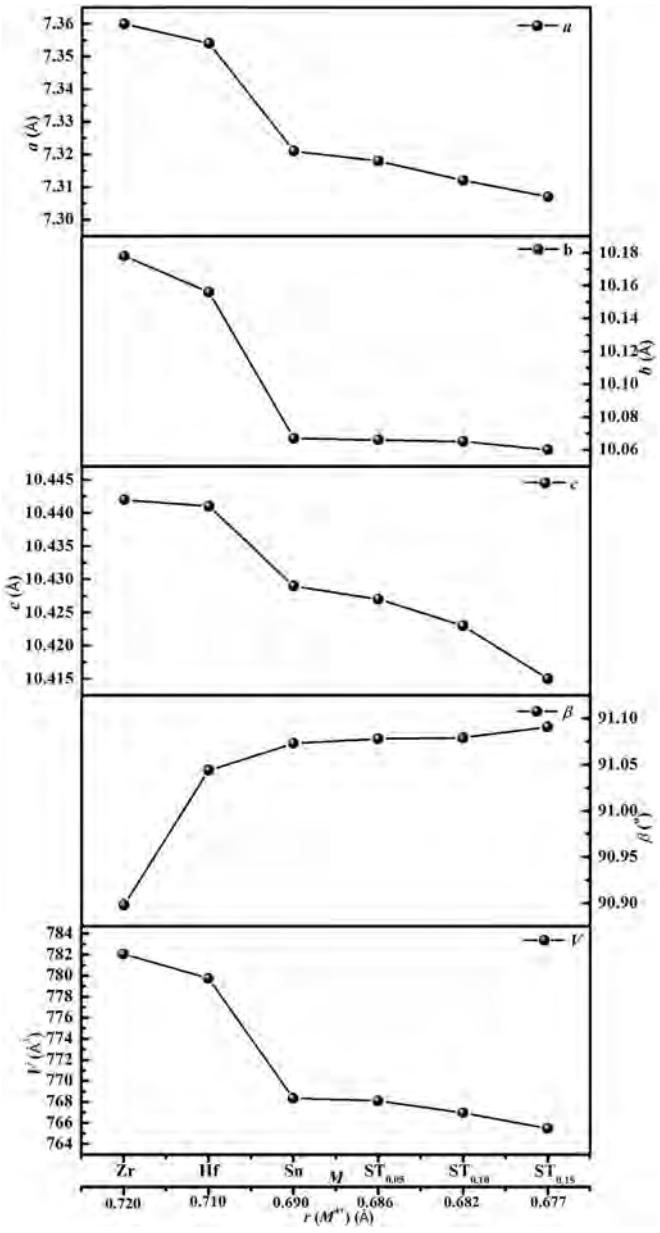

Fig. 2. The variation of lattice parameters of $Ca_3MSi_2O_9$ (M = Zr, Hf, $Sn_{1-x}Ti_x$; x = 0–0.15) ceramics with the M and r (M^{4+}).

[19] and EXPGUI [20] software. The microstructures of the $Ca_3MSi_2O_9$ samples were observed by scanning electron microscopy (SEM, Sirion 200, Netherlands), and the grain size distributions were obtained using Image J software. The ε_r and the unloaded $Q \times f$ value were measured at 12–14 GHz in the TE_{011} mode by Hakki and Coleman method [21] using a network analyzer (Agilent E8362B, Agilent Technologies, USA) and parallel silver boards. The τ_f value in the temperature range of 30–80 °C was calculated by Equation (3):

$$\tau_f = \frac{1}{f(T_0)} \frac{[f(T_1) - f(T_0)]}{T_1 - T_0} \quad (3)$$

where $f(T_1)$ and $f(T_0)$ represent the resonant frequency at T_1 (80 °C) and T_0 (30 °C), respectively.

3. Results and discussion

Fig. 1 shows the XRD patterns of $Ca_3MSi_2O_9$ (M = Zr, Hf, $Sn_{1-x}Ti_x$; x = 0–0.40) ceramics sintered at their optimum temperature and $[SnO_6]$–$[SiO_4]$ chain in $Ca_3MSi_2O_9$ (M = Sn) crystal structure. A single phase with monoclinic cuspidine structure and $P2_1/c$ space group can be obtained for $Ca_3MSi_2O_9$ (M = Zr, Hf, $Sn_{1-x}Ti_x$; x = 0–0.15). Whereas second phase $CaTiO_3$ is observed in $Ca_3MSi_2O_9$ ($M = Sn_{1-x}Ti_x$; x = 0.20–0.40), as shown in Fig. 1(a). This result indicates that the maximum solubility of $Ca_3Sn_{1-x}Ti_xSi_2O_9$ is located between 0.15 and 0.20. Rietveld refinement using GSAS was performed to analyze the crystal structure of $Ca_3MSi_2O_9$ (M = Zr, Hf, $Sn_{1-x}Ti_x$; x = 0–0.40) ceramics. Fig. 1(b) shows the crystal structure of $Ca_3SnSi_2O_9$ ceramics. The unit cell of which contains two $[SnO_6]$–$[SiO_4]$ chains composed of the $[SnO_6]$ octahedron and $[Si_2O_7]$ groups (Fig. 1(c)). The Rietveld discrepancy factors, such as Rp, Rwp, goodness of fit (χ^2) values, and lattice parameters of $Ca_3MSi_2O_9$ (M = Zr, Hf, $Sn_{1-x}Ti_x$; x = 0–0.40) are shown in Table 1 and Fig. 2. The Rietveld discrepancy factors in Table 1 show that the Rietveld refinement results are reliable. The lattice parameters a, b, c and unit-cell volumes V generally decrease when M changes from Zr to $Sn_{0.85}Ti_{0.15}$, corresponding to the decreasing of ionic radius (r^{4+}_{Zr} = 0.720 Å, r^{4+}_{Hf} = 0.710 Å, r^{4+}_{Sn} = 0.690 Å, r^{4+}_{Ti} = 0.605 Å; CN = 6) [17]. However, unlike the other lattice parameters, the β value which represents the angle between a and c in unit cell increases linearly, indicating that the symmetry of crystal structure decreases with the decreasing ionic radius of M^{4+}.

The microstructures of $Ca_3MSi_2O_9$ (M = Zr, Hf, $Sn_{1-x}Ti_x$; x = 0–0.40) ceramics sintered at their optimum temperature were observed using SEM, as shown in Fig. 3. All these images reveal a well-densified microstructure with uniform grain size and little porosity, except for $Ca_3SnSi_2O_9$ (Fig. 3(c)). For the $Ca_3SnSi_2O_9$ specimen sintered at 1400 °C, a porous microstructure with a large number of pores is present on the surface, and no clear grains can be observed. The relative density of $Ca_3SnSi_2O_9$ still has 96.6% (Table 2), so the pores may be caused by the Sn evaporation on the surface at high temperature [22]. When the Sn is partially substituted by Ti, the pores decrease remarkably. The average grain size of $Ca_3MSi_2O_9$ (M = Zr, Hf, $Sn_{1-x}Ti_x$; x = 0–0.40) ceramics is illustrated in Fig. 3, showing that the average grain size takes on the increasing tendency from 2.85 μm (M = Zr) to 4.20 μm ($M = Sn_{0.60}Ti_{0.40}$).

Table 2 presents the optimum sintering temperature, observed densities, relative densities, and microwave dielectric properties of $Ca_3MSi_2O_9$ (M = Zr, Hf, $Sn_{1-x}Ti_x$; x = 0–0.40) ceramics. The samples were prepared in a wide temperature range and only the best sample was selected for further investigation. All the samples are observed to possess high relative densities (approximately 98.0%). The relative permittivity and absolute value of τ_f decreases initially and then increases with the changing of M from larger Zr to smaller $Sn_{0.60}Ti_{0.40}$. However, the variation of $Q \times f$ value has an opposite trend comparing with relative permittivity as a function of M. It should be noted that the τ_f value approaches to near zero while the M is $Sn_{0.70}Ti_{0.30}$, which makes it a promising candidate for temperature-stable millimeter-wave devices.

In order to explain the variation tendency of microwave dielectric properties in single phase area, structural data are used to calculate some parameters, such as $\varepsilon_{r\text{-cal}}$, bond valence and relative covalence of M site. As for multi-phase area, the variation tendency of microwave dielectric properties is mainly affected by the second phase ($CaTiO_3$) and explained by mixing-rule (Lichtenecker empirical rule). The influence of porosity on ε_r can be eliminated by the following equation [23]:

$$\varepsilon_{r-obs} = \varepsilon_{r-\exp}(1 + 1.5P) \quad (4)$$

where P is the porosity and can be calculated by:

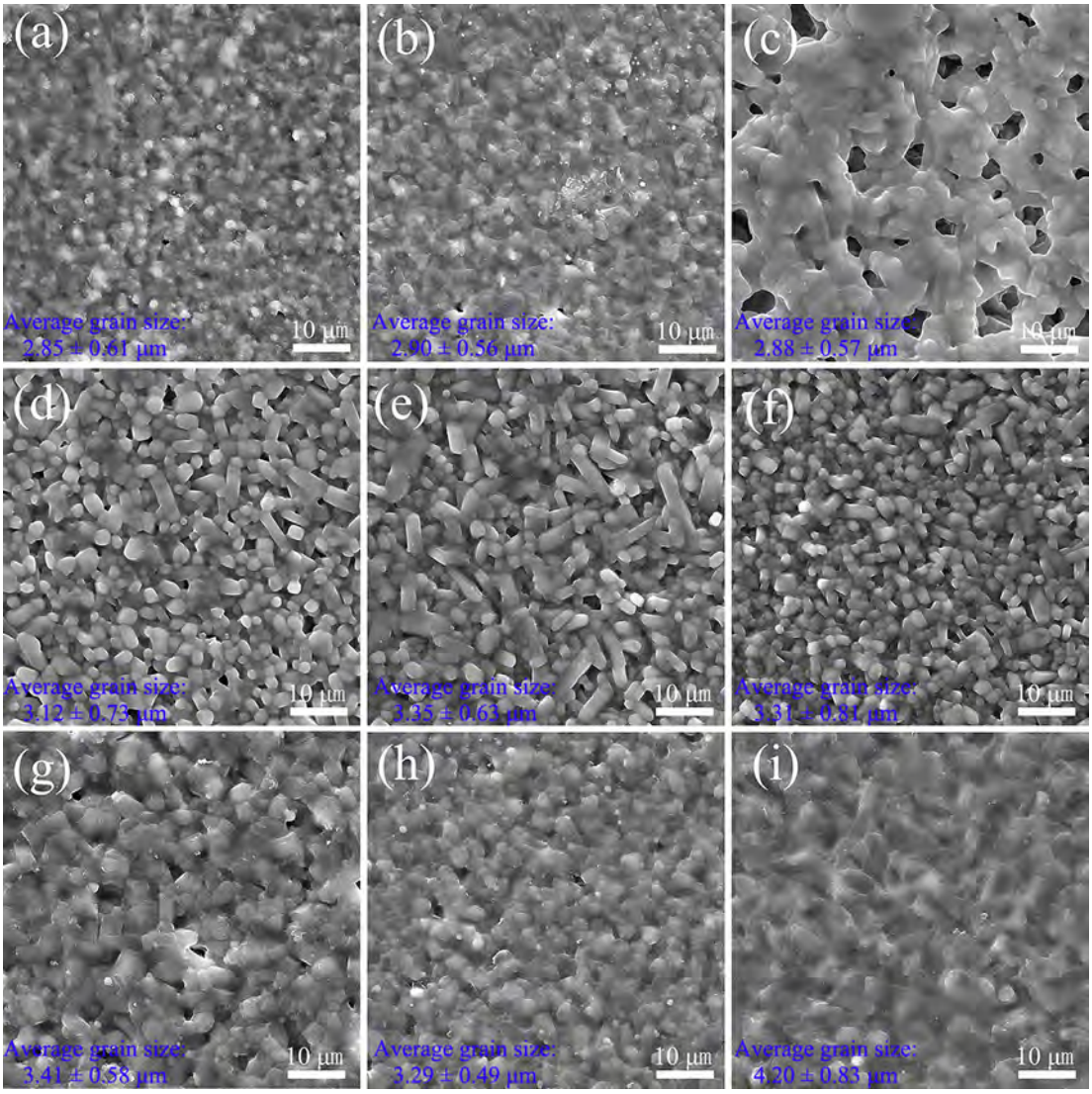

Fig. 3. Scanning electron micrographs and average grain size (insert) of $Ca_3MSi_2O_9$ (M = Zr, Hf, $Sn_{1-x}Ti_x$; x = 0–0.40) ceramics sintered at their optimum temperature: (a) M = Zr, 1375 °C; (b) M = Hf, 1375 °C; (c) M = Sn, 1400 °C; (d) $M = Sn_{0.95}Ti_{0.05}$, 1350 °C; (e) $M = Sn_{0.90}Ti_{0.10}$, 1350 °C; (f) $M = Sn_{0.85}Ti_{0.15}$, 1325 °C; (g) $M = Sn_{0.80}Ti_{0.20}$, 1350 °C; (h) $M = Sn_{0.70}Ti_{0.30}$, 1325 °C; (i) $M = Sn_{0.60}Ti_{0.40}$, 1350 °C.

Table 2
Sintering temperature (T_{sint}), observed densities (ρ_{obs}), relative densities (ρ_{rel}), and microwave dielectric properties of $Ca_3MSi_2O_9$ (M = Zr, Hf, $Sn_{1-x}Ti_x$; x = 0–0.40) ceramics.

Phase Composition	M	T_{sint} (°C)	ρ_{obs} (g/cm^3)	ρ_{rel} (%)	$\varepsilon_{r\text{-}exp}$	$\varepsilon_{r\text{-}obs}$	$\varepsilon_{r\text{-}cal}$	$Q \times f$ (GHz)	τ_f (ppm/°C)
CMS	Zr	1375	3.44 ± 0.03	98.3 ± 0.8	10.51 ± 0.05	10.87	7.92	44399 ± 549	−51.9 ± 2.0
	Hf	1375	4.19 ± 0.03	98.7 ± 0.7	10.27 ± 0.01	10.47	7.86	45017 ± 1741	−46.9 ± 1.6
	Sn	1400	3.67 ± 0.08	96.6 ± 1.2	8.80 ± 0.05	9.24	8.03	70944 ± 1169	−43.9 ± 1.0
	$Sn_{0.95}Ti_{0.05}$	1350	3.72 ± 0.02	98.7 ± 0.6	9.12 ± 0.06	9.29	8.04	72840 ± 1568	−41.0 ± 0.8
	$Sn_{0.90}Ti_{0.10}$	1350	3.73 ± 0.01	99.6 ± 0.2	9.30 ± 0.10	9.35	8.08	67117 ± 273	−40.1 ± 0.6
	$Sn_{0.85}Ti_{0.15}$	1325	3.70 ± 0.01	99.4 ± 0.2	9.50 ± 0.05	9.59	8.13	63694 ± 1579	−39.1 ± 0.4
CSS–CT	$Sn_{0.80}Ti_{0.20}$	1350	3.66 ± 0.05	97.9 ± 0.8	9.87 ± 0.08	10.19	–	52856 ± 1046	−29.4 ± 1.1
	$Sn_{0.70}Ti_{0.30}$	1325	3.73 ± 0.05	98.0 ± 0.8	11.07 ± 0.03	11.41	–	42400 ± 812	−5.1 ± 0.7
	$Sn_{0.60}Ti_{0.40}$	1350	3.75 ± 0.04	98.2 ± 0.7	12.34 ± 0.07	12.67	–	33840 ± 974	+26.4 ± 1.1

$\varepsilon_{r\text{-}exp}$: the measured value of ε_r; $\varepsilon_{r\text{-}obs}$: the correction value of ε_r; $\varepsilon_{r\text{-}cal}$: the calculated value of ε_r.

$$P = 1 - \rho_{rel} \tag{5}$$

Relative permittivity of $Ca_3MSi_2O_9$ (M = Zr, Hf, $Sn_{1-x}Ti_x$; x = 0–0.15) ceramics are also calculated by the total ionic polarizability of individual ions (α_D^T) and molar volume (V_m) according to Clausius-Mossotti equation [24,25]:

$$\varepsilon_{r-cal} = \frac{1 + 2b\alpha_D^T/V_m}{1 - b\alpha_D^T/V_m} \tag{6}$$

where $b = 4\pi/3$. The total ionic polarizability (α_D^T) of $Ca_3MSi_2O_9$ (M = Zr, Hf, $Sn_{1-x}Ti_x$; x = 0–0.15) can be calculated with the additive rule:

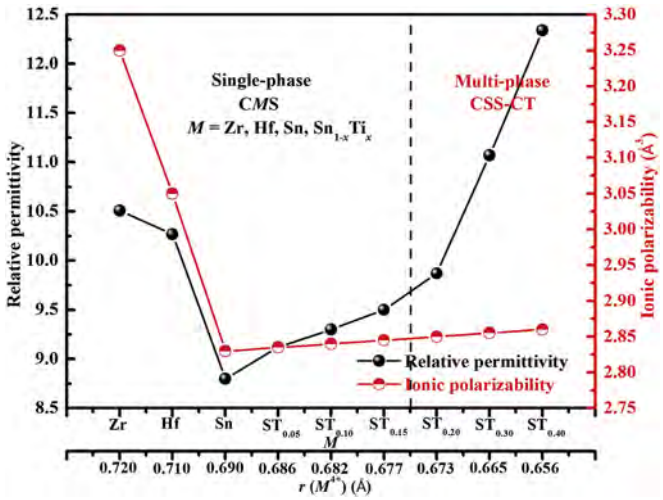

Fig. 4. The variation of relative permittivity and the ionic polarizability with the *M* and *r* (M^{4+}).

$$\alpha_D^T = 3\alpha\left(Ca^{2+}\right) + \alpha\left(M^{4+}\right) + 2\alpha\left(Si^{4+}\right) + 9\alpha\left(O^{2-}\right) \quad (7)$$

where $\alpha(Ca^{2+})$, $\alpha(M^{4+})$, $\alpha(Si^{4+})$ and $\alpha(O^{2-})$ are the ionic polarizability of Ca^{2+}, M^{4+}, Si^{4+} and O^{2-}, respectively.

The observed ($\varepsilon_{r\text{-obs}}$) and calculated ($\varepsilon_{r\text{-cal}}$) values of relative permittivity are listed in Table 2. The variation of $\varepsilon_{r\text{-exp}}$ and $\varepsilon_{r\text{-obs}}$ presents the same trend. However, because of the Clausius-Mossotti equation is more suitable for cubic or isotropic materials than low symmetry materials [26], the calculated $\varepsilon_{r\text{-cal}}$ is much smaller than $\varepsilon_{r\text{-obs}}$.

The variation of relative permittivity ($\varepsilon_{r\text{-exp}}$) and the ionic polarizability with the *M* are shown in Fig. 4. The variation tendency of $\varepsilon_{r\text{-exp}}$ is similar to that of ionic polarizability, especially in the single-phase area. This finding means that the variation of relative permittivity in single phase area is dominated by ionic polarizability of M^{4+} rather than the grain size or pores. In multi-phase area, the relative permittivity increases sharply with the increase of $CaTiO_3$ second phase. For multi-phase ceramics, the relative permittivity can be calculated from the Lichtenecker empirical rule [27]:

$$\ln \varepsilon_{r-cal} = V_1 \ln \varepsilon_{r-1} + V_2 \ln \varepsilon_{r-2} \quad (8)$$

where V_1 and V_2 are the volume fractions of CSS and CT; $\varepsilon_{r\text{-}1}$ and $\varepsilon_{r\text{-}2}$ are the relative permittivity of the CSS and CT, respectively. The volume fraction is calculated from the weight fraction, which is obtained from the refinement result. The relative permittivity of CSS and CT is $\varepsilon_{r\text{-}1} = 9.50$ and $\varepsilon_{r\text{-}2} = 170$ [28], respectively. Table 3 shows the weight fractions (*Wt.F*), volume fractions (*V.F*) and microwave dielectric properties of $Ca_3MSi_2O_9$ ($M = Sn_{1-x}Ti_x$; $x = 0.20$–0.40) (CSS–CT) composite. It is found that the calculated relative permittivity agrees well with the experimental value.

The quality factor ($Q \times f$) of $Ca_3MSi_2O_9$ ($M = Zr$, Hf, $Sn_{1-x}Ti_x$; $x = 0$–0.15) ceramics with the change of *M* (decreasing ionic radius of M^{4+}) are shown in Fig. 5. The $Q \times f$ increases initially and then decreases linearly, and the maximum $Q \times f$ value (72840 GHz) is obtained at $M = Sn_{0.95}Ti_{0.05}$. In general, the quality factor of microwave dielectric ceramics depends on intrinsic loss and extrinsic loss. The intrinsic losses are determined by absorptions of phonon oscillation and the extrinsic losses are dominated by many factors, such as second phase, porosity and grain size [3]. It is obvious that the quality factor of single phase area depends on intrinsic losses and the multiphase area is determined by $CaTiO_3$ second phase.

Many structural factors, such as bond valence, packing fraction, and relative covalence affect the $Q \times f$ value [9,29,30]. For $Ca_3MSi_2O_9$ ($M = Zr$, Hf, $Sn_{1-x}Ti_x$; $x = 0$–0.15), the bond valence of *M* site is calculated by the following equations [31,32]:

$$V_i = \sum_j v_{ij} \quad (9)$$

$$v_{ij} = \exp\left\{\frac{R_{ij} - d_{ij}}{n}\right\} \quad (10)$$

where R_{ij} is the bond valence parameter, d_{ij} is the bond length between the *i* and *j* atoms, and *n* is a constant of 0.37 Å. The bond lengths d_{ij} are obtained by refinement results and shown in Table S1.

The bond strength (*S*) is defined as the ratio of bond valence sum of cation and its coordination number, and the relationship among the bond strength (*S*), covalence (f_c) and relative covalence are given by the following equations [29]:

$$f_c = gS^m \quad (11)$$

$$\text{Relative Covalence}\ (\%) = \frac{f_c}{S} \times 100 \quad (12)$$

where *g* and *m* are the empirical parameters [32], which are dependent on the core electrons.

As shown in Fig. 5, the correlations between $Q \times f$ and *M* in the single phase area nearly reveal the same trend similar to those between relative covalence of *M* site and *M*, indicating that the relative covalence of *M* site plays a dominant role in controlling the $Q \times f$ value of $Ca_3MSi_2O_9$ ($M = Zr$, Hf, $Sn_{1-x}Ti_x$; $x = 0$–0.15). A similar correlation between $Q \times f$ value and relative covalence is also observed in $Ca_3Zr_{1-x}Sn_xSi_2O_9$ and $Ca_{1-x}Cd_xMoO_4$ solid solutions [9,29].

In multi-phase region, the $Q \times f$ value displays a linear variation, which is in good agreement with the empirical model for multi-phase ceramics (Table 3), and the model is described by the following equation [33]:

Table 3
Weight fractions (*Wt.F*), volume fractions (*V.F*) and microwave dielectric properties of $Ca_3MSi_2O_9$ ($M = Sn_{1-x}Ti_x$; $x = 0.20$–0.40) (CSS–CT) composite.

M	*Wt.F* (%)		*V.F* (%)		ε_r		$Q \times f$ (GHz)		τ_f (ppm/°C)	
	CSS	CT	CSS	CT	exp	cal	exp	cal	exp	cal
$Sn_{0.80}Ti_{0.20}$	98.09	1.91	98.20	1.80	9.87 ± 0.08	9.59	52856 ± 1046	59376	−29.4 ± 1.1	−29.8
$Sn_{0.70}Ti_{0.30}$	94.59	5.41	94.90	5.10	11.07 ± 0.03	10.57	42400 ± 812	45711	−5.1 ± 0.7	−4.0
$Sn_{0.60}Ti_{0.40}$	90.37	9.62	90.90	9.10	12.34 ± 0.07	11.88	33840 ± 974	35740	+26.4 ± 1.1	+28.1

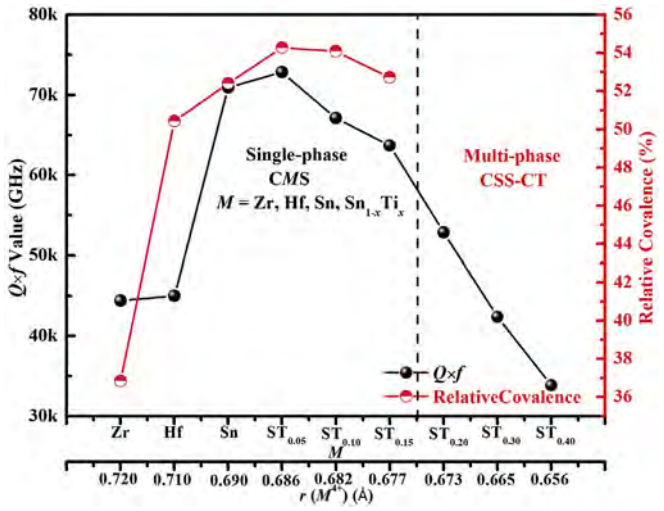

Fig. 5. The variation of $Q \times f$ value and the relative covalence of M site with the M and r (M^{4+}).

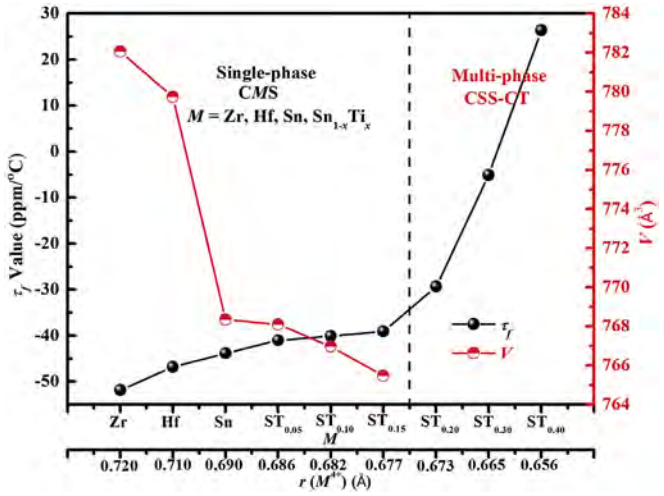

Fig. 6. The variation of τ_f value and the unit-cell volume with the M and r (M^{4+}).

$$\frac{1}{Q_f} = \frac{V_1}{(Q_f)_1} + \frac{V_2}{(Q_f)_2} \tag{13}$$

where $(Q_f)_1$ and $(Q_f)_2$ are the quality factors of the CSS and CT, respectively.

Fig. 6 shows the variation of τ_f value and the unit-cell volume with the M. Lee et al. [34] suggested that the unit-cell volume is inversely proportional to the lattice energy for a material family with a same lattice structure. In single phase area, the variation of τ_f has an opposite trend compared with unit-cell volume. Small unit-cell volume represents high lattice energy. Furthermore, high lattice energy means high stability of structure and temperature stability.

In two-phase composite ceramics, the τ_f can be described as [35]:

$$\tau_f = V_1(\tau_f)_1 + V_2(\tau_f)_2 \tag{14}$$

where $(\tau_f)_1$ and $(\tau_f)_2$ are the τ_f values of CSS and CT [27], respectively. The calculated τ_f values are shown in Table 3, and a near zero τ_f value is achieved for $M = Sn_{0.70}Ti_{0.30}$.

4. Conclusions

$Ca_3MSi_2O_9$ (M = Zr, Hf, $Sn_{1-x}Ti_x$; $x = 0$–0.40) microwave dielectric ceramics with low relative permittivity have been prepared via solid-state reaction process. A single phase with monoclinic cuspidine structure and $P2_1/c$ space group is obtained for $Ca_3MSi_2O_9$ (M = Zr, Hf, $Sn_{1-x}Ti_x$; $x = 0$–0.15). However, for $M = Sn_{1-x}Ti_x$ ($x = 0.20$–0.40), $CaTiO_3$ occurs as the second phase. For single phase region, the variation tendency of ε_r value is similar to that of ionic polarizability, which decreases initially and then increases linearly. The $Q \times f$ value is dependent on the relative covalence of M-site cations, and both of them reach the maximum value at $M = Sn_{0.95}Ti_{0.05}$. The variation of τ_f value is opposite to unit-cell volume. In multiphase region, the experimental microwave dielectric properties are consistent with the calculated results, meeting the mixing-rule. The highest $Q \times f$ value of 72840 GHz is obtained for $M = Sn_{0.85}Ti_{0.15}$, and near zero τ_f value is achieved for $M = Sn_{0.70}Ti_{0.30}$, which possesses the microwave dielectric properties of $\varepsilon_r = 11.07$, $Q \times f = 42400$ GHz, and $\tau_f = -5.1$ ppm/°C.

Acknowledgements

This work was supported by the National Natural Science Foundation of China (NSFC-51572093, 51772107, and 61771215). The authors are grateful to the Analytical and Testing Center, Huazhong University of Science and Technology, for SEM analyses.

Appendix A. Supplementary data

Supplementary data related to this article can be found at https://doi.org/10.1016/j.jallcom.2018.04.044.

References

[1] Z.Y. Zou, Z.H. Chen, X.K. Lan, W.Z. Lu, B. Ullah, X.H. Wang, W. Lei, Weak ferroelectricity and low-permittivity microwave dielectric properties of $Ba_2Zn_{(1+x)}Si_2O_{(7+x)}$ ceramics, J. Eur. Ceram. Soc. 37 (2017) 3065–3071.
[2] H.F. Zhou, X.H. Tan, J. Huang, N. Wang, G.C. Fan, X.L. Chen, Phase structure, sintering behavior and adjustable microwave dielectric properties of $Mg_{1-x}Li_{2x}Ti_xO_{1+2x}$ solid solution ceramics, J. Alloys Compd. 696 (2017) 1255–1259.
[3] H.C. Xiang, L. Fang, W.S. Fang, Y. Tang, C.C. Li, A novel low-firing microwave dielectric ceramic $Li_2ZnGe_3O_8$ with cubic spinel structure, J. Eur. Ceram. Soc. 37 (2017) 625–629.
[4] H. Taniguchi, A. Kuwabara, J. Kim, Y. Kim, H. Moriwake, S. Kim, T. Hoshiyama, T. Koyama, S. Mori, M. Takata, H. Hosono, Y. Inaguma, M. Itoh, Ferroelectricity driven by twisting of silicate tetrahedral chains, Angew. Chem. Int. Ed. 52 (2013) 8088–8092.
[5] C. Thieme, H. Görls, C. Rüssel, $Ba_{1-x}Sr_xZn_2Si_2O_7$–A new family of materials with negative and very high thermal expansion, Sci. Rep. 5 (2015) 18040.
[6] S.P. Wu, C. Jiang, Y.X. Mei, W.P. Tu, Synthesis and microwave dielectric properties of Sm_2SiO_5 ceramics, J. Am. Ceram. Soc. 95 (2012) 37–40.
[7] Y.M. Lai, C.Y. Hong, L.C. Jin, X.L. Tang, H.W. Zhang, X. Huang, J. Li, Temperature stability and high-Qf of low temperature firing Mg_2SiO_4–Li_2TiO_3 microwave dielectric ceramics, Ceram. Int. 43 (2017) 16167–16173.
[8] H.W. Chen, H. Su, H.W. Zhang, T.C. Zhou, B.W. Zhang, J.F. Zhang, X.L. Tang, Low-temperature sintering and microwave dielectric properties of $(Zn_{1-x}Co_x)_2SiO_4$ ceramics, Ceram. Int. 40 (2014) 14655–14659.
[9] A. Kan, H. Ogawa, H. Ohsato, Synthesis and crystal structure–microwave Dielectric property relations in Sn-substituted $Ca_3(Zr_{1-x}Sn_x)Si_2O_9$ solid solutions with cuspidine structure, Jpn. J. Appl. Phys. 46 (2007) 7108–7111.
[10] T. Tsunooka, M. Androu, Y. Higashida, H. Sugiura, H. Ohsato, Effects of TiO_2 on sinterability and dielectric properties of high-Q forsterite ceramics, J. Eur. Ceram. Soc. 23 (2003) 2573–2578.
[11] Y.P. Guo, H. Ohsato, K.I. Kakimoto, Characterization and dielectric behavior of willemite and TiO_2-doped willemite ceramics at millimeter-wave frequency, J. Eur. Ceram. Soc. 26 (2006) 1827–1830.
[12] N.H. Nguyen, J.B. Lim, S. Nahm, J.H. Paik, J.H. Kim, Effect of Zn/Si ratio on the microstructural and microwave dielectric properties of Zn_2SiO_4 ceramics, J. Am. Ceram. Soc. 90 (2007) 3127–3130.

[13] Y.C. Chen, J.M. Liou, M.Z. Weng, H.M. You, K.C. Chang, Improvement microwave dielectric properties of Zn_2SnO_4 ceramics by substituting Sn^{4+} with Ti^{4+}, Ceram. Int. 40 (2014) 10337–10342.
[14] J. Zhang, R.Z. Zuo, Effects of Zr substitution on the microstructure and microwave dielectric properties of $Li_2Zn(Ti_{1-x}Zr_x)_3O_8$ ceramics, J. Mater. Sci. Mater. Electron. 26 (2015) 9219–9224.
[15] J. Varghese, T. Joseph, M.T. Sebastian, $ZrSiO_4$ ceramics for microwave integrated circuit applications, Mater. Lett. 65 (2011) 1092–1094.
[16] J. Varghese, T. Joseph, K.P. Surendran, T.P.D. Rajan, M.T. Sebastian, Hafnium silicate: a new microwave dielectric ceramic with low thermal expansivity, Dalton Trans. 44 (2015) 5146–5152.
[17] R.D. Shannon, Revised effective ionic radii and systematic studies of interatomic distances in halides and chalcogenides, Acta Crystallogr. A 32 (1976) 751–767.
[18] H.M. Rietveld, A profile refinement method for nuclear and magnetic structures, J. Appl. Crystallogr. 2 (1969) 65–71.
[19] A.C. Larson, R.B. Von Dreele, General Structure Analysis System (GSAS), Los Alamos National Laboratory Report LAUR, 1994, pp. 86–748.
[20] B.H. Toby, EXPGUI, a graphical user interface for GSAS, J. Appl. Crystallogr. 34 (2001) 210–213.
[21] B.W. Hakki, P.D. Coleman, A dielectric resonant method of measuring inductive capacitance in the millimeter range, IRE. Trans. Microwave Theory Technol. 8 (1960) 402–410.
[22] S.P. Wu, D.F. Chen, Y.X. Mei, Q. Ma, Synthesis and microwave dielectric properties of $Ca_3SnSi_2O_9$ ceramics, J. Alloys Compd. 521 (2012) 8–11.
[23] G.K. Choi, J.R. Kim, S.H. Yoon, K.S. Hong, Microwave dielectric properties of scheelite (A = Ca, Sr, Ba) and wolframite (A = Mg, Zn, Mn) AMoO4 compounds, J. Eur. Ceram. Soc. 27 (2007) 3063–3067.
[24] R.D. Shannon, Dielectric polarizabilities of ions in oxides and fluorides, J. Appl. Phys. 73 (1993) 348–366.
[25] M.T. Sebastian, Dielectric Materials for Wireless Communication, Elsevier, 2010.
[26] X.Q. Song, W.Z. Lu, X.C. Wang, X.H. Wang, G.F. Fan, R. Muhammad, W. Lei, Sintering behaviour and microwave dielectric properties of $BaAl_{2-2x}(ZnSi)_xSi_2O_8$ ceramics, J. Eur. Ceram. Soc. (2017). https://doi.org/10.1016/j.jeurceramsoc.2017.10.053.
[27] H. He, Y. Xu, A unified equation for predicting the dielectric constant of a two phase composite, Appl. Phys. Lett. 104 (2014), 062906.
[28] J.S. Kim, C.I. Cheon, H.J. Kang, C.H. Lee, K.Y. Kim, S. Nam, J.D. Byun, Crystal structure and microwave dielectric properties of $CaTiO_3$–$(Li_{1/2}Nd_{1/2})TiO_3$–$(Ln_{1/3}Nd_{1/3})TiO_3$ (Ln = La, Dy) ceramics, Jpn. J. Appl. Phys. 38 (1999) 5633.
[29] S.D. Rama Rao, S. Roopas Kiran, V.R.K. Murthy, Correlation between structural characteristics and microwave dielectric properties of scheelite $Ca_{1-x}Cd_xMoO_4$ solid solution, J. Am. Ceram. Soc. 95 (2012) 3532–3537.
[30] E.S. Kim, B.S. Chun, R. Freer, R.J. Cernik, Effects of packing fraction and bond valence on microwave dielectric properties of $A^{2+}B^{6+}O_4$ (A^{2+}: Ca, Pb, Ba; B^{6+}: Mo, W) ceramics, J. Eur. Ceram. Soc. 30 (2010) 1731–1736.
[31] N.E. Brese, M. O'keeffe, Bond-valence parameters for solids, Acta Crystallogr. B 47 (1991) 192–197.
[32] I.D. Brown, R.D. Shannon, Empirical bond-strength-bond-length curves for oxides, Acta Crystallogr. A 29 (1973) 266–282.
[33] J. Zhang, R.Z. Zuo, Y. Cheng, Relationship of the structural phase transition and microwave dielectric properties in $MgZrNb_2O_8$–TiO_2 ceramics, Ceram. Int. 42 (2016) 681–7689.
[34] H.J. Lee, K.S. Hong, S.J. Kim, I.T. Kim, Dielectric properties of MNb_2O_6 compounds (where M = Ca, Mn, Co, Ni, or Zn), Mater. Res. Bull. 32 (1997) 847–855.
[35] H.R. Zheng, S.H. Yu, L.X. Li, X.S. Lyu, Z. Sun, S.L. Chen, Crystal structure, mixture behavior, and microwave dielectric properties of novel temperature stable $(1-x)MgMoO_4$–$xTiO_2$ composite ceramics, J. Eur. Ceram. Soc. 37 (2017) 4661–4665.